Optical constants of cubic GaN/GaAs(001): Experiment and modeling

Martín Muñoz,[a] Y. S. Huang,[b] and Fred H. Pollak[c]
Physics Department and New York Center for Advanced Technology in Ultrafast Photonic Materials and Applications, Brooklyn College of the City University of New York, Brooklyn, New York 11210

Hui Yang
State Key Laboratory on Integrated Optoelectronics and National Research Center for Optoelectronic Technology, Institute of Semiconductors, Chinese Academy of Sciences, Beijing 100083, People's Republic of China

(Received 30 September 2002; accepted 4 December 2002)

The optical constants $\varepsilon(E)=\varepsilon_1(E)+i\varepsilon_2(E)$ of unintentionally doped cubic GaN grown on GaAs(001) have been measured at 300 K using spectral ellipsometry in the range of 1.5–5.0 eV. The $\varepsilon(E)$ spectra display a structure associated with the critical point at E_0 (direct gap) and some contribution mainly coming from the E_1 critical point. The experimental data over the entire measured spectral range (after oxide removal) has been fit using the Holden–Muñoz model dielectric function [M. Muñoz *et al.*, J. Appl. Phys. **92**, 5878 (2002)]. This model is based on the electronic energy-band structure near critical points plus excitonic and band-to-band Coulomb-enhancement effects at E_0, $E_0+\Delta_0$ and the E_1, $E_1+\Delta_1$, doublet. In addition to evaluating the energy of the E_0 critical point, the binding energy (R_1) of the two-dimensional exciton related to the E_1 critical point was estimated using the effective mass/**k·p** theory. The line shape of the imaginary part of the cubic-GaN dielectric function shows excitonic effects at room temperature not withstanding that the exciton was not resolved. © *2003 American Institute of Physics.* [DOI: 10.1063/1.1540725]

I. INTRODUCTION

Wide band gap GaN-based materials are of interest from both applied and fundamental perspectives. Most of the GaN research has been devoted to studies of the hexagonal phase, however the metastable cubic phase of (*c*) GaN has some attractive advantages for device fabrication like easy cleavage and higher carrier mobility.[1–3] Structures based on *c*-GaN materials have been used for light emitting diodes[4] and showed its potential for lasers applications.[5–7] However, in spite of its fundamental and applied significance, relatively little work has been reported on the optical properties related to the electronic band. Some authors have performed measurements of the *c*-GaN dielectric function but not modeled the experimental results,[8] meanwhile others[9–11] modeled the optical constants not including continuum exciton contributions, i.e., band-to-band Coulomb enhancement effects (BBCEs) at E_0, $E_0+\Delta_0$, E_1, $E_1+\Delta_1$ critical points (CPs).

In this article we report a room temperature spectroscopic ellipsometry (SE) investigation of $\varepsilon(E)$ of unintentionally doped *c*-GaN in the photon energy range of 1.5–5.0 eV. A structure associated with E_0 CP and some contribution from higher energy CPs was observed. The experimental data over the entire measured spectral range (after oxide removal) has been fit using the Holden–Muñoz model dielectric function.[12] This model is based on the electronic energy-band structure near these CPs plus discrete and continuum excitonic effects at E_0, $E_0+\Delta_0$, E_1, and $E_1+\Delta_1$. In addition to evaluating the energy of the E_0 CP, we calculate the binding energy R_1 of the two-dimensional exciton related to the E_1, $E_1+\Delta_1$ CPs using effective mass/**k·p** theory.[13,14]

II. EXPERIMENTAL DETAILS

The *c*-GaN unintentionally doped sample studied was grown on a (001) GaAs substrate by metalorganic chemical vapor deposition. TEGa, NH_3, and H_2 were used as the Ga source, the N source, and carrier gas, respectively. During the growth process, a buffer layer was first grown on the substrate at 550 °C, then the cubic GaN film about 0.5 μm thick was deposited on the buffer layer at 820 °C. The flow rate of NH_3 is 200 sccm while the flow rate of TEGa is 50 sccm. Based on resistivity measurements the *n*-type background carrier concentration was estimated to be $n \sim 10^{15}$ cm^{-3}. The optical data in the range of 1.5–5.0 eV were taken using a JY-Horiba variable angle phase-modulated ellipsometer. The sample was measured with both 65° and 70° incidence angles. To remove the surface oxide we performed an etching procedure based on HCl, which is effective in reducing the native oxide of hexagonal GaN.[15] Details of this procedure are given in Ref. 16, except in this study the etch was a 1:1 mixture of HCl: methanol followed by a quick rinse in methanol and a spray of de-ionized water.

In order to obtain the dielectric function from the experimental ellipsometric angles the data analysis requires several steps, the first step of which is to determine the layer thick-

[a]Author to whom correspondence should be addressed; present address: Chemistry Dept., City College of the City University of New York, Convent Ave. at 138th St., New York, NY 10031; Electronic mail: mmunoz@sci.ccny.cuny.edu
[b]Permanent address: Dept. of Electronic Engineering, National Taiwan University of Science and Technology, Taipei 106, Taiwan.
[c]Also at the Graduate School and University Center of the City University of New York, New York, NY 10036; electronic mail: fhpbc@cunyvm.cuny.edu

ness. This value was determined from the interference fringes observed below the fundamental band gap, which are periodic in the product of the refractive index times the layer thickness divided by the wavelength. For this purpose, we assumed a Sellmeier model[17] for the behavior of the index of refraction in this transparent region. Next, using a multilayer ellipsometric analysis program and assuming sharp interfaces, our system was modeled using this thickness and the real and imaginary components of dielectric constant that best explained the experimental data for both angles; this analysis was performed sequentially for each wavelength within the program. We repeated this process for different assumed thickness, close to that previously determined, until we found a thickness and optical constants that minimized the residual error.

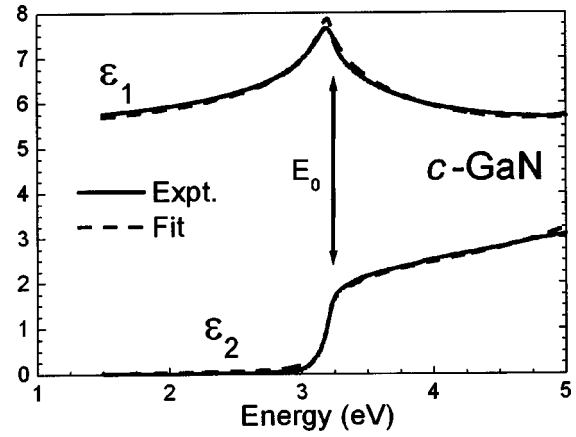

FIG. 1. Solid and dashed lines are the experimental and fit values, respectively, of the real (ε_1) and imaginary (ε_2) components of the complex dielectric function for *c*-GaN.

III. EXPERIMENTAL RESULTS AND THEORETICAL MODEL

The solid lines in Fig. 1 show the experimental values of the real $[\varepsilon_1(E)]$ and imaginary $[\varepsilon_2(E)]$ components of the dielectric function, respectively, as a function of the photon energy. In ε_2 spectrum there is an absorption edge around 3.2 eV, and some structure coming from high order transitions.

The experimental data over the entire measured spectral range (after oxide removal) have been fit using the Holden–Muñoz model[12] dielectric function is which is based on the electronic energy-band structure near these CPs plus excitonic and band-to-band Coulomb-enhancement effects at E_0, $E_0+\Delta_0$, and the E_1, $E_1+\Delta_1$, doublet.

In the direct-gap zincblende-type semiconductor *c*-GaN the spin–orbit interaction splits the highest-lying Γ_{15}^{ν} valence band into Γ_8^{ν} and Γ_7^{ν} (splitting energy Δ_0).[18] The corresponding lowest-lying transitions at $\mathbf{k}=0$ [three-dimensional (3D) M_0] are labeled $E_0[\Gamma_8^{\nu}(\Gamma_{15}^{\nu})-\Gamma_6^{c}(\Gamma_1^{c})]$ and $E_0+\Delta_0[\Gamma_7^{\nu}(\Gamma_{15}^{\nu})-\Gamma_6^{c}(\Gamma_1^{c})]$, respectively. The second direct gap transitions in this material is associated with a 2D M_0 CP $E_1[L_{4,5}^{\nu}(L_3^{\nu})-L_6^{c}(L_1^{c})$ or $\Lambda_{4,5}^{\nu}(\Lambda_3^{\nu})-\Lambda_6^{c}(\Lambda_1^{c})]$.[18]

The data near the E_0 band gap were fit to a function which contains Lorentzian-broadened (a) discrete excitonic (DE) and (b) 3D M_0 BBCE contributions. References 19 and 20 have demonstrated that even if the E_0 exciton is not resolved, the Coulomb interaction still affects the band-to-band line shape. Thus, $\varepsilon_2(E)$ is given by[12]

$$\varepsilon_{2,E_0}(E)=\mathrm{Im}\left\{\frac{A}{E^2}\left[\begin{array}{l} 2R_0\left(\dfrac{1}{(E_0-R_0)-E-i\Gamma_0^{\mathrm{ex}}}+\dfrac{1}{(E_0-R_0)+E+i\Gamma_0^{\mathrm{ex}}}\right) \\ +\displaystyle\int_{-\infty}^{\infty}\left(\frac{\theta(E'-E_0)}{1-e^{-2\pi z_1(E')}}-\frac{\theta(-E'-E_0)}{1-e^{-2\pi z_2(-E')}}\right)\frac{dE'}{E'-E-i\Gamma_0}\end{array}\right]\right\}, \tag{1}$$

where A is a constant, E_0 is the energy of the direct gap, R_0 is the effective Rydberg energy, Γ_0^{exc} is the broadening parameter of the first state of the exciton, Γ_0 is the broadening parameter for the band-to-band transition, $z_1(E)=\sqrt{R_0/(E-E_0)}$, $z_2(E)=\sqrt{R_0/(-E-E_0)}$, and $\theta(x)$ is the unit step function. In Eq. (1) the quantity $A\propto R_0^{1/2}\mu_0^{3/2}|P_0|^2$, where μ_0 is the reduced interband effective mass at E_0, and P_0 is the matrix element of the momentum between $\Gamma_8^{\nu}-\Gamma_6^{c}$. The terms in parentheses and under the integral in Eq. (1) correspond to the DE and BBCE contributions, respectively. Since the DE was not resolved, we took $\Gamma_0^{\mathrm{exc}}=\Gamma_0$.

For the E_1 CP, $\varepsilon_2(E)$ is written as[12]

$$\varepsilon_{2,E_1}(E)=\mathrm{Im}\left\{\frac{C_1}{E^2}\left[\begin{array}{l} 4R_1\left(\dfrac{1}{(E_1-R_1)-E-i\Gamma_{E_1}}+\dfrac{1}{(E_1-R_1)+E+i\Gamma_{E_1}}\right) \\ +\displaystyle\int_{-\infty}^{\infty}\left(\frac{\theta(E'-E_1)}{1-e^{-2\pi z_3(E')}}-\frac{\theta(-E'-E_1)}{1-e^{-2\pi z_4(-E')}}\right)\frac{dE'}{E'-E-i\Gamma_1}\end{array}\right]\right\}, \tag{2}$$

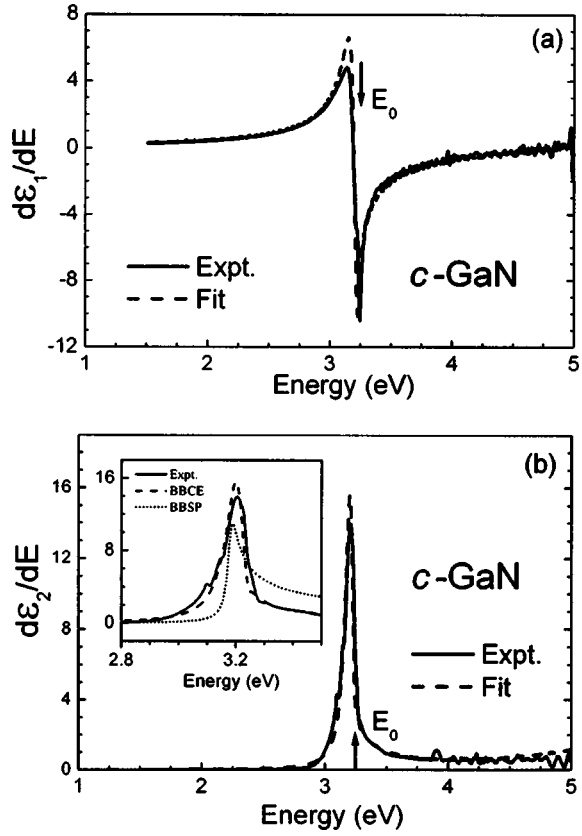

FIG. 2. Solid and dashed lines are the experimental and fit values, respectively, of: (a) $(d\varepsilon_1/dE)$ and (b) imaginary $(d\varepsilon_2/dE)$ for *c*-GaN. The solid, dashed, and dotted lines in the inset of (b) shows the ε_2 numerical derivative of the experimental data, fit using BBCE line shape and the parabolic one, respectively.

where C_1 is a constant, E_1 is the energy of the gap, R_1 is the 2D Rydberg energy, and Γ_{E_1} is the broadening parameter for both the exciton and band-to-band transition, $z_3(E)=\sqrt{R_1/(E-E_1)}$, $z_4(E)=\sqrt{R_1/(-E-E_1)}$, and $\theta(x)$ is the unit step function.

Equations (6) and (8) of Ref. 12 list relatively simple analytical expressions for $\varepsilon(E)$ for E_0, and E_1 based on Eqs. (1) and (2) presented above.

A constant $\varepsilon_{1\infty}$ was added to the real part of the dielectric constant to account for the vacuum plus contributions from higher-lying energy gaps (E_0', etc.).[12] This quantity should not be confused with the high frequency dielectric constant $\varepsilon(\infty)$.

In order to reduce the contributions of E_1 to $\varepsilon_2(E)$ below the fundamental gap E_0 we have introduced a linear cutoff for $\varepsilon_2(E)$, obtaining the corrected imaginary dielectric $\varepsilon_{2,\mathrm{co}}$

$$\varepsilon_{2,\mathrm{co}}(E)=\varepsilon_2(E)\frac{E-E_0}{E_{\mathrm{co}}-E_0}, \tag{3}$$

where E_{co} is the cutoff energy and E_0 is the direct band gap. ε_1 was corrected by a numerical Kramers–Kronig analysis of Eq. (3). The total dielectric function employed in this work is given by one term of the Eq. (1) type corresponding to E_0 CP, one of the Eq. (2) type for the E_1 CP, and $\varepsilon_{1\infty}$.

Our ellipsometer does not allow performing measurements at energies higher than 5.1 eV. For this reason we were not able to measure the E_1-R_1 transition, however, during our measurements some contribution of this transition was detected at energies smaller than 5 eV. In order to model this contribution we have used the value of E_1-R_1 from Refs. 18 and 23 as the fixed parameter. This value was also used to calculate R_1 using the **k·p** theory.[13,14] According to this approach

$$R_1=\frac{2\mu_\perp^* e^4}{\hbar^2\varepsilon_\infty^2},$$
$$\frac{1}{\mu_\perp^*}=\frac{1}{m_{c\perp}^*}-\frac{1}{m_{\nu\perp}^*}, \tag{4}$$

where $\mu_\perp^*$ is the perpendicular reduced interband effective mass related to E_1 and ε_∞ is the high-frequency dielectric function. From a three-band **k·p** formula the perpendicular conduction ($m_{c\perp}^*$) and valence ($m_{\nu\perp}^*$) effective masses (in units of the free-electron mass) are given by

$$\frac{1}{m_{c\perp}^*}=1+E_P\left(\frac{1}{E_1}+\frac{1}{E_1+\Delta_1}\right)$$
$$\frac{1}{m_{\nu\perp}^*}=1-\frac{E_P}{E_1}, \tag{5}$$

where E_P is proportional to the square of the magnitude of the matrix element of the perpendicular momentum between the corresponding conduction and valence bands. For *c*-GaN we have $\varepsilon_\infty=5.3$,[21] $E_P=24.6$ eV,[22] $E_1-R_1=7.0$ eV,[18,23] and $\Delta_0=17$ meV.[24] Using these values, Eqs. (4) and (5), and the two-thirds rule[25] we found $\Delta_1=11$ meV, $\mu_\perp^*=0.095$ (in units of the free electron mass), and $R_1=184$ meV.

The dotted curves in Fig. 1 are fits to the experimental data using the model described above. The arrow in the various figures indicate the fundamental band gap energy value

TABLE I. Values of the relevant parameters obtained in this experiment for the *c*-GaN sample. Also listed are energy gaps and the effective Rydberg energy R_0 from other investigations.

Parameter	This work	Previously reported
$A(\mathrm{eV}^{1.5})$	6.78 ± 0.01	⋯
E_0(eV)	3.25 ± 0.01	3.25[a]
		3.2[b]
		3.17[c]
		3.321[d]
R_0(meV)	27.0 ± 5.0	25–28[e]
		32[f]
Γ_0, Γ_0^{ex} (meV)	50.0 ± 5.0	
$C_1(\mathrm{eV}^2)$	116.5 ± 0.1	
E_1-R_1(eV)	7.0[g]	7.0[a,h,i]
R_1(meV)	184.0[g]	
Γ_1, Γ_1^{ex} (meV)	780.0 ± 50.0	
$\varepsilon_{1\infty}$	2.042 ± 0.005	
E_{co}(eV)	5.00 ± 0.01	

[a]Reference 23.
[b]Reference 11.
[c]Reference 9.
[d]Reference 24.
[e]Reference 34.
[f]Reference 35.
[g]Fixed.
[h]Incorrectly labeled E_1.
[i]Reference 18.

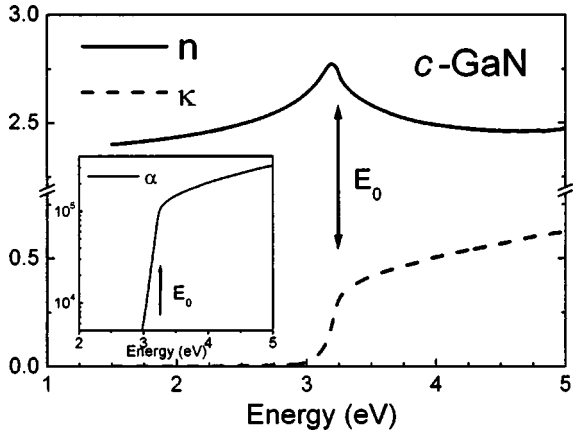

FIG. 3. Solid and dashed lines are the experimental values of the real n and imaginary κ components, respectively, of the complex index of refraction for c-GaN. The solid line in the inset is the experimental value of the absorption coefficient α for c-GaN.

obtained as a result of our fit. All relevant parameters are listed in Table I. The corresponding values of $d\varepsilon_1(E)/dE$ and $d\varepsilon_2(E)/dE$ for the experimental and fit spectra, obtained from a numerical derivative, are shown by the solid and dotted lines in Figs. 2(a) and 2(b), respectively. Overall there is very good agreement between experiment and theory for both the dielectric function (Fig. 1) and the first derivative [Figs. 2(a) and 2(b)].

IV. DISCUSSION OF RESULTS AND SUMMARY

The results of this experiment are in good agreement with prior studies of the optical constants of c-GaN.[8–11] Figure 1 correspond closely to the relevant data of Ref. 10 in the range of 1.5–3.7 eV. The real and imaginary components of the index of refraction n and k and the absorption coefficient α, displayed in Fig. 3, were obtained using our experimental data. Table I shows that the values of the energy gap E_0, obtained in this investigation, as well as the other parameters used in this work. The E_0 value is in good agreement with other selected experiments. There is some scatter in the experimental data, probably due to differences in sample quality, surface preparation, and/or line-shape analysis.

The optical constants ε_1 and ε_2 for c-GaN over an extended range have been investigated by a number of authors,[8–11] mainly using SE. However, Lin[8] did not model their results, References 9–11 used a model in which the E_0 CP is represented by only Lorenztian broadened band-to-band single-particle (BBSP) expressions, i.e., no DE. Petalas[9] modeled the E_1 CP by a Lorenztian function associated with a weighted average value of E_1 and E_2 CPs, meanwhile Köhler[10] used a simple harmonic oscillator for E_1.

As mentioned above the optical structure associated with the E_1 CP is primarily excitonic. References 9–11 did not include the BBCE contribution either at E_0 or E_1. Excitonic effects at the E_0 CP also must be included, even at room temperature. In the presence of a DE, the band-to-band E_0 line shape (within about 6–10 R_0) is changed from the BBSP square root (broadened) term to a three-dimensional BBCE expression, which has a line shape similar to a step function (broadened), as shown in Fig. 1, and also increases the amplitude of the absorption in relation to the BBSP expression.[12,25,26]

The inadequacy of the BBSP approach at E_0 is clearly demonstrated in the inset of Fig. 2(b), where the dotted line is a fit of the E_0 feature to the first derivative of a 3D M_0 BBSP expression. Note that the fit is quite asymmetric on the high-energy side, while the experimental curve is symmetric, consistent with a BBCE line shape. Thus, the inset of Fig. 2(b) demonstrates conclusively that even if the exciton is not resolved, the line shape is BBCE and not BBSP, in agreement with Refs. 19 and 20.

Also the nature of the BBCE line shape is clearly illustrated in Fig. 6 of Ref. 27, Figs. 2 and 3 of Ref. 28, and by Fig. 3 in Ref. 29. The deficiency of the BBSP model is also elucidated by Figs. 2 and 3 of Ref. 28 and Fig. 3 in Ref. 29, where they show that the only use of the BBSP and BBSP plus DE exciton line shapes is not adequate to fit the imaginary part of the dielectric function. In Fig. 3 of Ref. 29 the fit expressions for the DE plus BBSP are considerably lower than the experimental data, particularly for the 21 K measurement.

Table II of Ref. 12 presents the R_1 values for several semiconductors; from this it is possible to appreciate that there is a good trend between the experimental values and the **k·p** theory. More reliable theoretical values can now be obtained from the recent first-principles band structure calculations which include exciton effects.[30,31]

The ability to measure R_1 has considerable implications for band-structure calculations: both empirical[32] and first principles.[30,31] In the former case, band-structure parameters, e.g., pseudopotential form factors, are determined mainly by comparison with optical and modulated optical experiments, including the E_1, $E_1+\Delta_1$ features. Therefore, the band-to-band energies are too low by an amount R_1. Rohlfing and Louie have published a first-principles calculation of the optical constants of GaAs, including excitonic effects.[30] Using this formalism they have also calculated R_0. Their approach also makes it possible to evaluate R_1 from first principles.[33] Albrecht *et al.*[31] also have recently presented an *ab initio* approach for the calculation of excitonic effects in the optical spectra of semiconductors and insulators. However, to date they have presented results for only Si.

The consideration of the excitonic effects at E_0, $E_0+\Delta_0$, E_1 and $E_1+\Delta_1$ during the modeling of the dielectric function is a fundamental consideration as discussed in Ref. 12.

In summary, we have measured the room-temperature complex dielectric function of bulk c-GaN in the range of 1.5–5.0 eV using SE. The structure related to E_0 and some contribution mainly coming from E_1 CP has been observed. The experimental data over the entire measured spectral range has been fit using the Holden–Muñoz model for the dielectric function, which is based on the electronic energy-band structure near these CPs plus DE and BBCE effects at E_0, $E_0+\Delta_0$, E_1, and $E_1+\Delta_1$. In addition to determining the energy of E_0 CP, using the effective mass/**k·p** theory we have evaluated the 2D exciton binding energy R_1 (=184

meV). The line shape of the imaginary part of the *c*-GaN dielectric function and its derivative demonstrates clearly that excitonic effects, even at room temperature and with no exciton resolved, must be taken into account using a BBCE line shape and not a BBSP.

ACKNOWLEDGMENT

The authors M.M. and F.H.P. thank the New York State Science and Technology Foundation through its Centers for Advanced Technology program for support of this project.

[1] R. C. Powell, N. E. Lee, Y. W. Kim, and J. E. Greene, J. Appl. Phys. **73**, 189 (1993).
[2] H. Liu, A. C. Vrenkel, J. G. Kim, and R. M. Park, J. Appl. Phys. **74**, 6124 (1993).
[3] M. J. Paisley, Z. Sitar, J. B. Posthill, and R. F. Davis, J. Vac. Sci. Technol. A **7**, 701 (1989).
[4] H. Yang, L. X. Zheng, J. B. Li, X. J. Wang, D. P. Xu, and Y. T. Wang, Appl. Phys. Lett. **74**, 2498 (1999).
[5] R. Klann, O. Brandt, H. Yang, H. T. Grahn, and K. H. Ploog, Appl. Phys. Lett. **70**, 1076 (1997).
[6] J. Holst, L. Eckey, A. Hoffmann, I. Broser, B. Schöttker, D. J. As, D. Schikora, and K. Lischka, Appl. Phys. Lett. **72**, 1439 (1998).
[7] A. Nakadaira and H. Tanaka, Appl. Phys. Lett. **71**, 812 (1997).
[8] E. Lin, B. N. Sverdlov, S. Strite, H. Morkoc, and A. E. Drakin, Electron. Lett. **29**, 1759 (1993).
[9] J. Petalas, S. Logothetidis, S. Boultadakis, M. Alouani, and J. M. Wills, Phys. Rev. B **52**, 8082 (1995).
[10] U. Köhler, D. J. As, B. Schöttker, T. Frey, K. Lischka, J. Scheiner, S. Shokhovets, and R. Goldhahn, J. Appl. Phys. **85**, 404 (1999).
[11] T. Suzuki, H. Yaguchi, H. Okumura, Y. Ishida, and S. Yoshida, Jpn. J. Appl. Phys., Part 2 **39**, L497 (2000).
[12] M. Muñoz, T. M. Holden, F. H. Pollak, M. Kahn, D. Ritter, L. Kronik, and G. M. Cohen, J. Appl. Phys. **92**, 5878 (2002).
[13] Y. Petroff and M. Balkanski, Phys. Rev. B **3**, 3299 (1971).
[14] E. O. Kane, Phys. Rev. **180**, 852 (1969); in *Semiconductors and Semimetals*, Vol. 1, edited by R. K. Willardson and A. C. Beer (Academic, New York, 1966), p. 75.
[15] K. N. Lee, S. M. Donovan, B. Gila, M. Overberg, J. D. Mackenzie, C. R. Abernathy, and R. G. Wilson, J. Electrochem. Soc. **147**, 3087 (2000).
[16] T. Holden, P. Ram, F. H. Pollak, J. L. Freeouf, B. X. Yang, and M. C. Tamargo, Phys. Rev. B **56**, 4037 (1997).
[17] F. A. Jenkins and H. E. White, *Fundamentals of Optics*, 3rd ed. (McGraw–Hill, New York, 1957), p. 472.
[18] A. Rubio, J. Corkill, M. L. Cohen, E. L. Shirley, and S. G. Louie, Phys. Rev. B **48**, 11810 (1993).
[19] K. Wei, F. H. Pollak, J. L. Freeouf, D. Shvydka, and A. D. Compaan, J. Appl. Phys. **85**, 7418 (1999).
[20] F. H. Pollak, M. Muñoz, T. Holden, K. Wei, and V. M. Asnin, Phys. Status Solidi B **215**, 33 (1999).
[21] V. Yu. Davydov, A. V. Subashiev, T. S. Cheng, C. T. Foxon, I. N. Goncharuk, A. N. Smirnov, and R. V. Zolotareva, Solid State Commun. **104**, 397 (1997).
[22] A. T. Meney, E. P. O'Reilly, and A. R. Adams, Semicond. Sci. Technol. **11**, 897 (1996).
[23] S. Logothetidis, I. Petalas, M. Cardona, and T. D. Moustakas, Phys. Rev. B **50**, 18017 (1994).
[24] G. Ramirez-Flores, H. Navarro-Contreras, A. Lastras-Martínez, R. C. Powell, and J. E. Greene, Phys. Rev. B **50**, 8433 (1994).
[25] P. Y. Yu and M. Cardona, *Fundamentals of Semiconductors* (Springer, Heidelberg, 1996).
[26] F. Bassani and G. Pastori Parravicini, *Electronic States and Optical Transitions in Solids* (Pergamon, Oxford, 1975).
[27] C. H. Yan, H. Yao, J. M. Van Hove, A. M. Wowchak, P. P. Chow, and J. M. Zavada, J. Appl. Phys. **88**, 3463 (2000).
[28] C. C. Kim and S. Sivananthan, Phys. Rev. B **53**, 1475 (1996).
[29] S. Adachi, Phys. Rev. B **41**, 1003 (1990).
[30] M. Rohlfing and S. G. Louie, Phys. Rev. Lett. **81**, 2312 (1998).
[31] S. Albrecht, L. Reining, R. Del Sole, and G. Onida, Phys. Rev. Lett. **80**, 4510 (1998).
[32] M. L. Cohen and J. R. Chelikowsky, *Electronic Structure and Optical Properties of Semiconductors* (Springer, Berlin, 1989).
[33] Louie (private communication).
[34] J. Menniger, U. Jahn, O. Brandt, H. Yang, and K. Ploog, Phys. Rev. B **53**, 1881 (1996).
[35] Z. X. Liu, A. R. Goñi, K. Syassen, H. Siegle, C. Thomsen, B. Schöttker, D. J. As, and D. Schikora, J. Appl. Phys. **86**, 929 (1999).